

# Broadly tunable mid-infrared femtosecond optical parametric oscillator using all-solid-state-pumped periodically poled lithium niobate

Kent C. Burr and C. L. Tang

*Cornell University, Ithaca, New York 14853*

Mark A. Arbore and Martin M. Fejer

*Stanford University, Stanford, California 94305*

Received May 30, 1997

We describe a high-repetition-rate femtosecond optical parametric oscillator (OPO) that was broadly tunable in the mid infrared. The all-solid-state-pumped OPO was based on quasi-phase matching in periodically poled lithium niobate. The idler was tunable from approximately  $1.7\ \mu\text{m}$  to beyond  $5.4\ \mu\text{m}$ , with maximum average power levels greater than 200 mW and more than 20 mW of average power at  $5.4\ \mu\text{m}$ . We used interferometric autocorrelation to characterize the mid-infrared idler pulses, which typically had durations of 125 fs. This OPO had a pumping threshold as low as 65 mW of average pump power, a maximum conversion efficiency of  $>35\%$  into the near-infrared signal, a slope efficiency for the signal of approximately 60%, and a maximum pump depletion of more than 85%. © 1997 Optical Society of America

Mid-IR femtosecond pulses have potential applications for the study of dynamics in a variety of materials. Vibrational relaxations in molecules, intersubband transitions in quantum wells, and materials for use in lasers and detectors operating in the  $3\text{--}5\text{-}\mu\text{m}$  atmospheric transmission window can all be studied effectively with ultrashort mid-IR pulses. In this Letter we report on the generation of mid-IR pulses with an all-solid-state-pumped high-repetition-rate femtosecond (fs) optical parametric oscillator (OPO).

The most common techniques for the generation of high-repetition-rate mid-IR fs pulses are difference-frequency mixing and the use of a synchronously pumped OPO. Difference frequency of the signal and the idler output from Ti:sapphire-pumped OPO's produced fs pulses of between  $2.5$  and  $5.5\ \mu\text{m}$  (Ref. 1) but with maximum average power levels of only  $500\ \mu\text{W}$ . Mid-IR synchronously pumped fs OPO's based on  $\text{KTiOPO}_4$  and its isomorphs<sup>2–5</sup> were demonstrated, but they were limited to wavelengths shorter than  $\sim 4.1\ \mu\text{m}$ . Average power levels greater than 20 mW at  $5.2\ \mu\text{m}$  were obtained with  $\text{KNbO}_3$ .<sup>6</sup> The all-solid-state-pumped broadly tunable mid-IR fs OPO described in this Letter is based on quasi-phase matching<sup>7</sup> (QPM) in periodically poled lithium niobate (PPLN) and produced more than 20 mW of average power at  $5.4\ \mu\text{m}$ .

The experimental arrangement was similar to that described in Ref. 8, except that a ring cavity was used instead of a linear cavity. We used a pumping geometry with a small noncollinear angle between the pump and the signal so that the long-wavelength idler beam did not have to be transmitted through any of the cavity optics and optical isolation of the pump laser was unnecessary. The PPLN OPO was synchronously pumped at a repetition rate of 81 MHz by a mode-locked fs Ti:sapphire laser powered by a diode-pumped cw frequency-doubled Nd:YVO<sub>4</sub> laser (Spectra-Physics Millennia). The Ti:sapphire laser produced

nearly transform-limited pulses of  $\sim 90$ -fs duration, with average power levels of as much as 850 mW over the  $790\text{--}815\text{-nm}$  wavelength range used in this experiment. We used two optics sets and two PPLN crystals, which were antireflection coated on both sides with single layers of  $\text{SiO}_2$ , in the OPO to cover the tuning range. In both cases the signal was resonated in a ring cavity consisting of two 15-cm radius-of-curvature mirrors, a flat high reflector, a flat output coupler, and a four-prism (SF-14) sequence for dispersion compensation. Several different output couplers were used, with transmission varying from  $\sim 1\%$  to  $\sim 9\%$  over the tuning range of the OPO.

In a noncollinear fs OPO both temporal walk-off owing to the group-velocity mismatch (GVM) of the interacting pulses and spatial walk-off owing to the noncollinearity of the interacting beams can limit the effective interaction length in the crystal. Near degeneracy<sup>9</sup> the GVM between the pump pulses and signal and idler pulses was of the order of 300 fs/mm (signal-and-idler-leading pump),<sup>10</sup> resulting in a temporal walk-off length<sup>11</sup> of the order of  $330\ \mu\text{m}$  for  $\sim 100$ -fs pulse widths. Far from degeneracy, the GVM between pump and signal was reduced to as little as  $\sim 110$  fs/mm, but the GVM between signal and idler became as large as  $\sim 260$  fs/mm (signal-leading idler), resulting in a temporal walk-off length of  $\sim 900\ \mu\text{m}$  between the pump and the signal and  $\sim 380\ \mu\text{m}$  between the signal and the idler. For the focusing parameters ( $\sim 35\text{-}\mu\text{m}$  signal and pump waist radius) and the noncollinear angle (varied from  $\sim 1.0^\circ$  to  $\sim 1.6^\circ$  between pump and signal measured internal to the crystal) used in this experiment, near degeneracy the spatial walk-off length of  $\sim 550\ \mu\text{m}$  between signal and idler was much larger than the temporal walk-off length and, therefore, did not limit the interaction length. When we were trying to reach long idler wavelengths, however, the increasingly large angle between signal and idler (as large as  $9^\circ$  measured

internal to the crystal) resulted in a spatial walk-off length as small as  $\sim 220 \mu\text{m}$  between signal and idler. Thus, far from degeneracy the effective interaction length was limited by the spatial walk-off length, which was significantly shorter than the temporal walk-off length. In both cases a collinear geometry would allow for much tighter focusing without limiting the interaction length and would undoubtedly result in a lower threshold and higher output power levels.

The relatively short interaction length was compensated for by the extremely large  $d_{33}$  nonlinear coefficient of lithium niobate ( $\text{LiNbO}_3$ ) that was accessible by polarizing all three waves parallel to the  $z$  axis ( $e \rightarrow e + e$ ).<sup>12</sup> The ability of the PPLN fs OPO to generate sufficient gain for oscillation in a very short interaction length (a few hundred micrometers) allowed it to tolerate relatively large material absorption coefficients [as high as  $\sim 5 \text{ cm}^{-1}$  for the idler at  $5.4 \mu\text{m}$  (Ref. 13)] and, thus, to operate far into the IR-absorption edge of  $\text{LiNbO}_3$ .

Near degeneracy the short interaction length, the low GVM between signal and idler, and the low group-velocity dispersion at the signal and the idler wavelengths resulted in an extremely large phase-matching bandwidth<sup>11</sup> (several hundred nanometers). The temperature bandwidth was also extremely large (greater than  $100^\circ\text{C}$ ), making precise control of the crystal temperature unnecessary for a PPLN fs OPO.<sup>8</sup> Calculated<sup>10</sup> tuning curves, assuming perfect phase matching, are shown in Figs. 1(a) and 1(b). Experimentally, the OPO is subject to repetition-rate matching of the signal and the pump pulses, and the output power is dependent on the round trip loss and the phase-matching conditions. Repetition-rate matching is necessary for temporal overlap of the pump and the signal pulses and depends on cavity length and wavelength owing to group-velocity dispersion. The round-trip loss depends on the spectral characteristics of all the optics in the cavity. As a result of the extremely large phase-matching bandwidth, which is comparable with the bandwidth of the cavity optics, for a given pump wavelength and crystal temperature the signal wavelength can vary over hundreds of nanometers depending on the adjustment of the cavity length and the prism sequence, and the wavelength at which the maximum output power occurs is strongly dependent on the spectral characteristics of the specific output coupler that is used. Thus a quantitative comparison of experimental data with tuning curves in Fig. 1 would be meaningless. Our experimental observations agree with the calculated tuning curves in terms of accessible wavelength range and general tuning trends.

To reach the longest idler wavelengths, we used an optics set that was highly reflective from  $0.95$  to  $1.12 \mu\text{m}$  and a PPLN crystal that had a grating period of  $19.0 \mu\text{m}$ , was  $800 \mu\text{m}$  long (longer than the spatial walk-off length), and was antireflection coated for  $0.96 \mu\text{m}$ . A representative interferometric autocorrelation of the signal is shown in Fig. 1(c), with the corresponding spectrum shown in Fig. 1(d). Signal pulse widths were typically less than  $100 \text{ fs}$ . The idler

branch was tunable from approximately  $2.7$  to beyond  $5.4 \mu\text{m}$ . An idler spectrum, obtained when the idler was tuned to  $5.4 \mu\text{m}$ , is shown in Fig. 2(a), along with the background transmission in air. The bands in the transmission through air, which were responsible for the modulation in the idler spectrum, most likely were due to absorption by water vapor.<sup>14</sup> The average idler power at  $5.4 \mu\text{m}$  was more than  $20 \text{ mW}$  while pumping with  $\sim 630 \text{ mW}$  of Ti:sapphire power, corresponding to a quantum efficiency of greater than  $20\%$ . For comparison, we must emphasize that these results were achieved with an all-solid-state pump laser that produced significantly less power than is available from the argon-ion-pumped systems typically used for fs OPO's.<sup>2-6</sup> Figure 2(b) shows an interferometric autocorrelation of the idler beam, which did not include any dispersion-compensating elements, when the idler wavelength was  $\sim 5 \mu\text{m}$ . The corresponding pulse

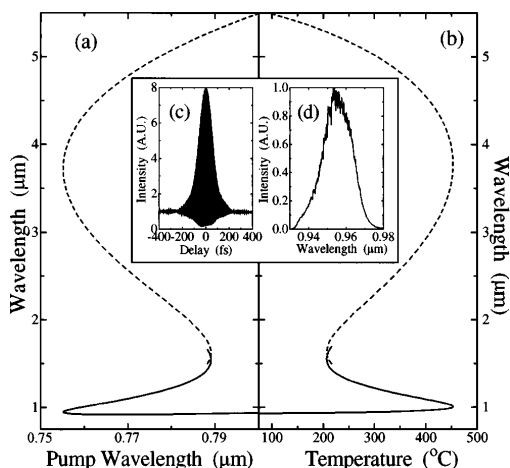


Fig. 1. Calculated tuning curves for the signal (solid) and the idler (dashed) with a QPM grating period of  $19.0 \mu\text{m}$  and an internal angle of  $1.14^\circ$  between pump and signal for (a) pump tuning at a temperature of  $150^\circ\text{C}$  and (b) temperature tuning at a pump wavelength of  $795 \text{ nm}$ . (c) Typical signal autocorrelation and (d) corresponding spectrum.

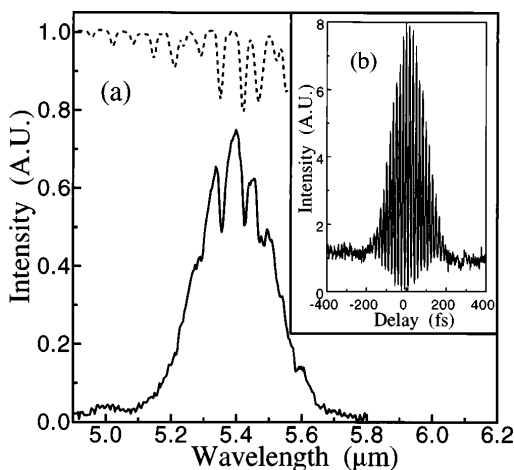


Fig. 2. (a) Idler spectrum (solid curve) and background transmission in air (dashed curve). (b) Typical interferometric autocorrelation of the idler when the wavelength was  $\sim 5 \mu\text{m}$ .

width is  $\sim 125$  fs, assuming a  $\text{sech}^2$  pulse shape. This autocorrelation was recorded with two-photon absorption in an InAs photodiode<sup>15</sup> (EG&G Judson J12-18C-R01M). By use of Si, Ge, and InAs photodiodes it was possible to record autocorrelations in all regions of the idler tuning range.

For operation closer to degeneracy, we used a second optics set that was highly reflective from 1.1 to 1.5  $\mu\text{m}$  and a PPLN crystal that had a grating period of 19.5  $\mu\text{m}$ , was 330  $\mu\text{m}$  long and was antireflection coated for 1.35  $\mu\text{m}$ . The idler branch was tunable from approximately 1.7 to 2.7  $\mu\text{m}$ . With the signal wavelength near 1.35  $\mu\text{m}$ , as much as 280 mW of average power was produced in the signal beam while pumping with 775 mW of Ti:sapphire power, corresponding to 36% power conversion efficiency from pump to signal (61% quantum efficiency). Under these conditions the pump was depleted by more than 85%, and the slope efficiency for the signal was  $\sim 60\%$ . More than 200 mW of average power was measured in the idler beam. By replacing the output coupler with a high reflector we reduced the round-trip loss to  $\sim 3.5\%$  and the threshold to  $\sim 65$  mW of average pump power.

Tuning was accomplished in several ways. Because of the large phase-matching bandwidth, simply changing the cavity length, at a constant crystal temperature and pump wavelength, resulted in tuning over more than 150 nm, limited by the output coupler bandwidth. Using multiple output couplers and changing the crystal temperature, which was always maintained above 75 °C, made it possible to tune over the entire bandwidth of the cavity mirrors. We also tuned the OPO either by changing the pump wavelength or by adjusting the noncollinear angle between the signal and the pump beams.

At long idler wavelengths, which experienced significant absorption within the crystal, the spatial modes of the second harmonic of the signal and the pump beams showed effects from thermal lensing. Photorefractive damage was also evident when appreciable levels of signal second harmonic were generated in the blue region of the visible spectrum. When operating with the signal in the 1.1–1.5- $\mu\text{m}$  region, we did not observe thermal lensing or photorefractive problems.

As is common with fs OPO's, in addition to the signal and the idler beams we also observed beams at several visible wavelengths corresponding to different combinations of second-harmonic generation, sum-frequency generation, and difference-frequency generation. When either second-harmonic generation from the signal or sum-frequency generation from pump and signal was quasi-phase matched by a higher-order wave vector from the QPM grating, the average power levels in these visible beams were of the order of 10% of the average pump power. We observed second-, third-, and fourth-order QPM of the second harmonic of the signal. For the sum frequency of pump and signal we observed third-, fourth-, and fifth-order QPM. Third-order QPM of the sum frequency of pump and signal was recently observed<sup>16</sup> in a picosecond PPLN OPO.

In conclusion, we have demonstrated an all-solid-state-pumped high-repetition-rate broadly tunable mid-IR femtosecond optical parametric oscillator based on quasi-phase matching in periodically poled lithium niobate. The idler was tunable from approximately 1.7  $\mu\text{m}$  to beyond 5.4  $\mu\text{m}$ , with more than 20 mW of average power at 5.4  $\mu\text{m}$ . We used interferometric autocorrelation to characterize the mid-IR pulses, which typically had a duration of  $\sim 125$  fs. When operating closer to degeneracy, this OPO had a low threshold, a slope efficiency of  $\sim 60\%$  for the signal beam, and a maximum pump depletion of more than 85%. We also observed efficient generation of visible pulses owing to higher-order QPM of second-harmonic and sum-frequency generation in the PPLN crystal.

We thank Spectra-Physics Lasers for the use of the Millennia and gratefully acknowledge assistance from Stephan Wielandy and Li Yang. This research was supported by the Joint Services Electronics Program, the National Science Foundation, and the Defense Advanced Research Projects Agency through the Center for Nonlinear Optical Materials.

## References

1. J. D. Kafka, M. L. Watts, J. W. Pieterse, and R. L. Herbst, *Appl. Phys. B* **60**, 449 (1995); A. Lohner, P. Kruck, and W. W. Ruhle, *Appl. Phys. B* **59** 211 (1994).
2. P. E. Powers, C. L. Tang, and L. K. Cheng, *Opt. Lett.* **19**, 1439 (1994).
3. G. R. Holtom, R. A. Crowell, and L. K. Cheng, *Opt. Lett.* **20**, 1880 (1995).
4. S. W. McCahon, S. A. Anson, D. J. Jang, and T. F. Boggess, *Opt. Lett.* **20**, 2309 (1995).
5. D. T. Reid, C. McGowan, M. Ebrahimzadeh, and W. Sibbett, *IEEE J. Quantum Electron.* **33**, 1 (1997).
6. D. E. Spence, S. Wielandy, C. L. Tang, C. Bosshard, and P. Günter, *Appl. Phys. Lett.* **68**, 452 (1996).
7. J. A. Armstrong, N. Bloembergen, J. Ducuing, and P. S. Pershan, *Phys. Rev.* **127**, 1918 (1962); M. M. Fejer, G. A. Magel, D. H. Jundt, and R. L. Byer, *IEEE J. Quantum Electron.* **28**, 2631 (1992).
8. K. C. Burr, C. L. Tang, M. A. Arbore, and M. M. Fejer, *Appl. Phys. Lett.* **70**, 3341 (1997).
9. Throughout this Letter when we refer to "near degeneracy" this includes signal wavelengths from approximately 1.2 to 1.5  $\mu\text{m}$ .
10. All calculations were made with Sellmeier equations from G. J. Edwards and M. Lawrence, *Opt. Quantum Electron.* **16**, 373 (1984).
11. See, e.g., S. A. Akhmanov, A. I. Kovrygin, A. P. Sukhorukov, and R. L. Byer, both in *Quantum Electronics*, H. Rabin and C. L. Tang, eds. (Academic, New York, 1975), Vol. 1B, pp. 472–586, 587–702.
12. For a discussion of the relative merits of PPLN for use in fs devices, see M. A. Arbore, M. M. Fejer, M. E. Fermann, A. Hariharan, A. Galvanauskas, and D. Harter, *Opt. Lett.* **22**, 13 (1997).
13. L. E. Myers, R. C. Eckardt, M. M. Fejer, R. L. Byer, and W. R. Bosenberg, *Opt. Lett.* **21**, 591 (1996).
14. G. Guelachvili and K. N. Rao, *Handbook of Infrared Standards* (Academic, New York, 1986).
15. Y. Takagi, T. Kobayashi, K. Yoshihara, and S. Imamura, *Opt. Lett.* **17**, 658 (1992).
16. S. D. Butterworth, P. G. R. Smith, and D. C. Hanna, *Opt. Lett.* **22**, 618 (1997).